Switching axial progenitors from producing trunk to tail tissues in vertebrate embryos

Arnon Dias Jurberg[1], Rita Aires[1], Irma Varela-Lasheras[1], Ana Nóvoa[1] and Moisés Mallo[1,2,#]

1 Instituto Gulbenkian de Ciência. Rua da Quinta Grande 6. 2780-156 Oeiras. Portugal
2 Department of Histology and Embryology, Faculty of Medicine, University of Lisbon, Lisbon, Portugal

Running title: control of trunk to tail transition

Key words: trunk to tail transition, Gdf11, Isl1, axial progenitors

#Correspondence to M. Mallo
Tel: +351-214464624
Fax: +351-214407970
e-mail: mallo@igc.gulbenkian.pt

ABSTRACT

The vertebrate body is made by progressive addition of new tissue from progenitors at the posterior embryonic end. Axial extension involves different mechanisms that produce internal organs in the trunk but not in the tail. We show that Gdf11 signaling is a major coordinator of the trunk to tail transition. Without Gdf11 signaling the switch from trunk to tail is significantly delayed and its premature activation brings the hindlimbs and cloaca next to the forelimbs, leaving extremely short trunks. *Gdf11* activity includes activation of *Isl1* to promote formation of the hindlimbs and cloaca-associated mesoderm as the most posterior derivatives of lateral mesoderm progenitors. *Gdf11* also coordinates reallocation of bipotent neuromesodermal progenitors from the anterior primitive streak to the tail bud, in part by reducing the retinoic acid available to the progenitors. Our findings provide a new perspective to understand the evolution of the vertebrate body plan.

INTRODUCTION

Vertebrates display a large diversity of body shapes and sizes. Despite such morphological variations, their primary body axis is always generated from head to tail through a similar principle, consisting of the progressive addition of new tissue at the posterior end of the embryo (reviewed in Stern et al., 2006; Wilson et al., 2009). This process requires a fine balance between the maintenance of progenitor pools and the continuous production of cells that form the different body structures. Cells leaving the axial progenitor pools at different stages during the elongation process execute patterning and differentiation programs that are specific to each particular axial level. Quantitative and qualitative differences in these general processes are the basis of vertebrate body shape diversity. One of the most important components of anterior-posterior (AP) regional variation is the portion of the postcranial body occupied by the neck, trunk, and tail. For instance, the prototypical snake's body has a very long trunk and rather short neck and tail. In contrast, birds exhibit long necks and reduced tails, whereas some lizards have fairly short necks and trunks, but very long tails. Thus, elucidating the mechanisms that control this regional organization is essential to understand the evolution of the vertebrate body plan.

The transition from trunk to tail is one of the key elements in AP organization of the vertebrate body. While the trunk holds most of the vital and reproductive organs, the tail is basically composed of vertebrae and its associated muscles. These differences reflect major changes in developmental mechanisms during axial extension. Embryologically, trunk tissues require extensive contributions from all three germ layers, including the lateral and intermediate mesoderm, which in concert with the endoderm originate the trunk-associated organs (Carlson, 1999). Conversely, tail tissues are mostly derived from the paraxial mesoderm and ectoderm. This means that the trunk to tail transition marks the posterior end of the endoderm, as well as of the lateral and intermediate mesoderm. Interestingly, this is associated with the induction of the hindlimb buds from the lateral mesoderm and with the activation of molecular programs in the ectoderm, hindgut endoderm, and ventral lateral mesoderm resulting in the production of the embryonic cloaca (Suzuki et al., 2009). The consequences of this embryological feature are still patent in the adult animal as the end of the trunk typically

correlates with the position of the cloaca and its derivatives, and of the hindlimbs, if the animal has them.

The trunk to tail transition is also associated with a switch in the mechanism guiding embryonic axial growth. Trunk formation is driven by a midline structure called the primitive streak (PS), in which ingressing cells from the epiblast generate the embryonic mesoderm and definitive endoderm (Psychoyos and Stern, 1996; Tam and Beddington, 1997; Wilson and Beddington, 1996). Conversely, caudal growth during tail formation is associated with the activity of the tail bud (Kanki and Ho, 1997; Schoenwolf, 1977). This change in the mode of axial growth involves the relocation of axial progenitors from the PS and adjacent areas of the epiblast to the caudal neural hinge (CNH) at the posterior end of the tail bud (Cambray and Wilson, 2002; 2007; Wilson and Beddington, 1996).

The mechanisms controlling the trunk to tail transition are largely unknown, despite their importance. As for other aspects of AP regional patterning, most of the studies on differences between the trunk and the tail have focused on their associated skeleton (reviewed by Mallo et al., 2009; 2010; Wellik, 2007). In the adult animal, the trunk typically expands through the thoracic and lumbar segments of the vertebral column, whereas the transition to the tail occurs through the sacrum and the tail itself is associated with caudal vertebrae. Regional specification of these skeletal segments results from the execution of distinct patterning programs during differentiation of the somitic mesoderm (reviewed by Mallo et al., 2009; 2010; Wellik, 2007). Although coordinated with the networks controlling other aspects of trunk and tail development, these mechanisms mostly operate within the paraxial mesoderm and cannot account for such transition. Indeed, a variety of genetic experiments in the mouse indicate that the embryo can undergo major patterning changes in their axial skeletons with very little or no obvious effects on hallmarks of the trunk to tail transition, such as the position of the hindlimbs (Carapuço et al., 2005; McIntyre et al., 2007; Vinagre et al., 2010; Wellik and Capecchi, 2003). There are a few mutant phenotypes, however, that are suggestive of a simultaneous alteration in several aspects of the trunk to tail transition. Those associated with the inactivation of Gdf11 signaling in mice are particularly interesting, as they produce a global anteriorization of the axial skeleton (Andersson et al., 2006; Essalmani

et al., 2008; McPherron et al., 1999; Oh et al., 2002; Szumska et al., 2008). Mutants for members of this pathway generally present 16-18 thoracic and 7-8 lumbar segments instead of the wild type 13 and 6 vertebrae, respectively. In these mutants, transformations in the axial skeleton are associated with a posterior displacement of the hindlimbs by about 6-8 vertebral units (Andersson et al., 2006; McPherron et al., 1999; Oh et al., 2002; Szumska et al., 2008).

Here, we show that Gdf11 signaling is a major regulator of the trunk to tail transition during vertebrate development. Whereas loss of *Gdf11* delays the specification of the cloaca and the induction of the hindlimbs, precocious activation of Gdf11 signaling in the epiblast using a constitutively active form of its receptor, $Alk5^{CA}$, produces a remarkable anteriorization of these structures, with a concomitant reduction in trunk length. Strikingly, by using different promoters, we show that this activity is required in the axial progenitors of the epiblast and not in the derived mesoderm. We present evidence that the switch from trunk to tail progenitors requires a combination of several processes. These include activation of *Isl1* in the progenitors for the lateral mesoderm, which results in the induction of the hindlimb buds and cloacal tissues. The regulation of *Isl1* expression by Gdf11 signaling seems to be mediated by direct control of a relevant enhancer of *Isl1* that is specifically active during this transition. Gdf11 signaling is also involved in the orderly relocation of the bipotent neuromesodermal (N-M) progenitors from the PS to the tail bud, a process that requires inactivation of retinoic acid signaling.

RESULTS

Loss of *Gdf11* delays trunk to tail transition in mice

Gdf11 mutant newborn animals present anterior homeotic transformations along the axial skeleton, with posterior displacement of the hindlimbs by 6 to 8 vertebrae (McPherron et al., 1999). Analysis of these mutants at embryonic day (E)11.5 revealed that the hindlimb buds were indeed more posteriorly located, producing an increased interlimb (trunk) region by 5 or 6 somites when compared to wild type embryos (Fig. 1A,B). At this stage, *Gdf11* mutant hindlimbs were visibly smaller than those of their wild type littermates (Fig. 1A,B), which contrasted with their normal morphology at E18.5 (Fig. S1A,B). Embryonic staging based on hindlimb morphology (Boehm et al., 2011) revealed that the

hindlimbs of E10.5 and E11.5 *Gdf11* mutant embryos corresponded to those of younger wild type embryos by about 6 and 17 hours, respectively (Fig. 1C). This observation raised the possibility that hindlimb specification is delayed in *Gdf11* mutant embryos. Consistent with this hypothesis, analysis of *Tbx4* expression, an early hindlimb marker (Gibson-Brown et al., 1996), revealed that the hindlimb fields were first identified at an axial level 5-6 somites more posterior in *Gdf11* mutants than in wild type embryos (Fig. 1D,E). These results suggest that *Gdf11* is involved in establishing the position at which the hindlimb is induced along the AP axis.

Given the correlation between the hindlimbs and the trunk to tail transition, the above results suggest that Gdf11 signaling plays a fundamental role in setting this transition. Consistent with this, other hallmarks of the trunk to tail transition were also posteriorly displaced in *Gdf11* mutants, compared with wild type littermates. In particular, we examined both endodermal (*Shh* and *Fgf8* expression) (Fig. 1F-I) and mesodermal (*Isl1* and *Raldh2* expression) (Figs 1J,K and S1C-F) components of the developing cloaca. In *Gdf11* mutants, these markers were expressed next to the posterior end of the hindlimb buds, similar to what was observed in wild type embryos, revealing that the primordium of the cloaca was also located at a more posterior absolute axial level. In addition to the posterior displacement of the hindlimb buds and the cloaca, formation of other tissues and structures typically associated with the trunk was caudally extended in *Gdf11* mutant embryos. For instance, expression of *Pax2* and *Raldh2* revealed a posterior elongation of the intermediate mesoderm, which is the precursor of the urogenital tract (Figs 1L,M and S1C,D). Similarly, the visceral lateral mesoderm extended to more caudal levels, as evidenced by the expression of *Wnt2* (Fig. 1N,O). Altogether, these results show that the trunk to tail transition was posteriorly displaced in *Gdf11* mutants and that this was associated with a concomitant extension of trunk-associated tissues to cover the body up to the cloacal level. They also indicate that the alterations observed in the axial skeleton of these mutants (McPherron et al., 1999) are just one manifestation of a more global deregulation of AP patterning processes.

Alk5 activation in the epiblast anteriorizes the trunk to tail transition

To explore whether *Gdf11* signaling is able to dominantly control the trunk to tail transition, we took a gain of function approach in mouse embryos. Genetic and biochemical experiments revealed that Gdf11 first binds Acvr2b to form a complex that then activates Alk5 (also known as Tgfbr1) to initiate a signaling cascade mediated by Smad2 (Andersson et al., 2006; Ho et al., 2010; Liu, 2006; Oh et al., 2002). It has been suggested that the start of *Gdf11* functional activity is determined by Alk5 availability, which in axial tissues seems to start at around E9.0 (Andersson et al., 2006). Therefore, for our gain of function experiments we produced transgenic embryos expressing a constitutively active version of Alk5 ($Alk5^{CA}$), which signals independently of the ligand (Wieser et al., 1995).

We first expressed $Alk5^{CA}$ using an enhancer element of the *Cdx2* gene (*Cdx2P-*$Alk5^{CA}$ transgenics), which has been shown to drive expression in the posterior epiblast and PS (Benahmed et al., 2008; Gaunt et al., 2005). Activity of this enhancer was detected in the progenitors for neural and mesodermal tissues posterior to the forelimb bud level, although the forelimb progenitors were themselves mostly not targeted by the enhancer (Fig. S2A-C). *Cdx2P-*$Alk5^{CA}$ embryos exhibited strong phenotypes affecting posterior embryonic growth (n=22 out of 37 transgenics), which could be classified in two groups. The most severe phenotypes (n=12) included a drastic axial truncation leaving very little tissue posterior to the forelimbs (Fig. S2D,E). This phenotype did not permit the analysis of patterning processes in the trunk region of these embryos. Another group of *Cdx2P-*$Alk5^{CA}$ embryos (n=10), however, exhibited milder phenotypes, extending their AP axis beyond the forelimb bud level. These embryos had short bodies but contained clearly recognizable hindlimbs and tails, and preserved fairly normal overall regional organization (Fig. 2). Interestingly, their hindlimbs were located very close to the forelimbs, leaving extremely short trunks spanning 0-6 misshapen somites in contrast to the typical 12-13 somites observed in wild type E10.5 embryos. The position of the anteriorized hindlimbs was often asymmetric and in one transgenic embryo the hindlimb buds were duplicated (Fig. 2L). In these embryos the cloaca also developed in a more anterior location, maintaining its relative anatomical position with respect to the hindlimbs (Fig. 2E-H). Globally, these phenotypes were essentially the opposite to those

observed in *Gdf11* mutant embryos, thus reinforcing the important role of Gdf11/Alk5 signaling in establishing the position of the trunk to tail transition. We were not able to recover any affected *Cdx2P-Alk5*^{CA} transgenic at a stage that allowed direct evaluation of AP patterns in the axial skeleton. However, the anterior expression boundaries of *Hoxa9* and *Hoxc10* at E10.5 were anteriorized, maintaining their position relative to the hindlimb bud (Fig. 2I-L), indicating altered AP patterns also in the paraxial mesoderm and neural tube. This observation is consistent with previous Gdf11 gain of function experiments in chicken embryos (Liu, 2006). Altogether, these results indicate the existence of a global and coordinated posteriorization of the body plan of *Cdx2P-Alk5*^{CA} transgenic embryos that involves tissues from all germ layers.

It has been reported that the *Cdx2* enhancer used in these experiments is active in both the axial progenitor-containing posterior epiblast and in the underlying mesodermal compartments (Benahmed et al., 2008). To evaluate if the phenotypes observed in the *Cdx2P-Alk5*^{CA} transgenics derived from Alk5 activity in the epiblast or in the mesodermal compartments, we overexpressed *Alk5*^{CA} in the paraxial mesoderm using the *Dll1*-msd enhancer (Beckers et al., 2000) and in the lateral mesoderm using a *Hoxb6* enhancer (Becker et al., 1996). We could not identify any abnormality in any of these transgenics (n=21 and n=22, respectively), indicating that the phenotypes observed in *Cdx2P-Alk5*^{CA} transgenics are most probably derived from the activation of Alk5 signaling in the epiblast and not in the derived mesodermal compartments.

Taken together, our results indicate that Gdf11/Alk5 signaling is a key modulator of the transition from trunk to tail in the mouse. In addition, they show that this signaling is required in the epiblast and it is therefore very probable that it primarily acts on the axial progenitors. This suggests that Gdf11 signaling might be involved in the modulation of the different functional changes in these progenitors driving their switch from making trunk to tail tissues.

Altered tail bud organization in *Gdf11* mutant embryos

A typical characteristic of *Gdf11* mutant skeletons is their truncation at the sacral/caudal level (McPherron et al., 1999). In midgestation embryos, we found that the tails of *Gdf11* mutant embryos exhibited variable phenotypes, typically being distally thinner than in

wild type embryos and duplicated in a proportion of them (Fig. S3A,D). *T* (*Brachyury*) was expressed at the tip of both tail tips (Fig. S3D), indicating that the duplicated tail might have resulted from a splitting of the posterior organizing area. Therefore, we investigated the transition from PS to tail bud in *Gdf11* mutant embryos. At E9.5 we already observed deviations from the normal *T* expression pattern in *Gdf11*$^{-/-}$ embryos, as transcripts for this gene were distributed in a broader domain that extended anteriorly through the prospective tail tip (Fig. 3A,B). This broadening was progressively resolved into a distinct domain, which appeared to segregate by E10.5 (Fig. 3C,D). In these embryos, distal thinning of the tail bud started to become evident. At this stage, expression of other genes functionally associated with the posterior growth area at the tail tip, like *Cdx2*, *Fgf8*, and *Wnt3a*, also exhibited abnormal expression to different extents (Fig. 3I-N). At E11.5 we could observe two or three distinct *T*-positive domains along the ventral side of the tails of *Gdf11* mutants, from their tip to the posterior border of the hindlimb buds, even in embryos without split tails (Fig. 3E,F). However, at this stage, expression of the other markers was restricted to the posterior end of the tail or present at differential levels in the two tail tips when the embryos had a split tail (Figs 1I and S3E-H). Interestingly, in all *Gdf11*$^{-/-}$ embryos analyzed at E11.5 we found an ectopic *T*-expression domain located next to the hindlimbs, regardless of whether or not their tails were split (Figs 3F and S3D). This group of cells was negative for other tested markers of the posterior organizing area (Fig. S3F,H). Surprisingly, although these cells were positive for *T*, we could not identify ectopic formation of mesodermal tissues in the caudal end of the *Gdf11* mutants. Instead, we observed ectopic neural tissue ventrally located outside the vertebral column (Fig. S3I,J), an observation consistent with previous analysis of both *Gdf11* and *Pcsk5* mutant embryos (Szumska et al., 2008). It has been established that the bipotent N-M progenitors in the tail bud take a neural fate in the absence of Wnt3a activity (Martin and Kimelman, 2012). Therefore, it is possible that the ectopic *T* domain represents a fraction of such progenitors that failed to become incorporated into the CNH and differentiated into neural tissue due to the absence of Wnt3a.

Altogether, these results are consistent with an abnormal PS to CNH transition in the absence of Gdf11 activity, in which the pool of axial progenitors normally fated to

form the CNH becomes split into several domains instead of a single region at the tail tip. The split tail might be produced when the number (or specific characteristics) of progenitors trapped halfway through the tail is large enough to generate another tail bud, eventually creating a secondary ventral tail.

Gdf11 is required to reduce RA levels during the transition from PS to CNH

It has been reported that the tail truncation of *Gdf11*$^{-/-}$ fetuses can be partially rescued by pharmacological inhibition of retinoic acid (RA) signaling (Lee et al., 2010). The timing of the effective treatment fits with the PS to CNH transition, which raises the possibility that the tail rescue may result from the recovery of this process. To test this possibility, we analyzed how treatment with the RA inhibitor AGN193109 affected tail bud development in *Gdf11* mutants. Notwithstanding some degree of variability (probably resulting from different efficiencies of the treatment), the tails of these embryos at E10.5 were consistently longer and thicker than those of untreated *Gdf11*$^{-/-}$ embryos, some of them resembling the tails of wild type embryos (Fig. 3G). In addition, we did not find any embryo with a split tail. *T* expression in the caudal end of these embryos also showed some variability but in most embryos it was restricted to the tail tip without ectopic *T*-expressing domains (Fig. 3G). These results indicate that inhibition of RA signaling produces a significant reversion of the abnormalities observed in the PS to CNH transition typically observed in *Gdf11* mutants, placing RA signaling as a key element causing the abnormal behavior of axial progenitors in *Gdf11* mutant embryos.

To further explore this hypothesis, we performed the complementary experiment and analyzed the effect of increased RA levels at the time of the PS to CNH transition on the axial progenitors of *Gdf11*$^{-/-}$ embryos. At E11.5, RA-treated mutants had variable tail malformations that were always stronger than those observed in non-treated *Gdf11* mutant embryos (Fig. 3H). Tail morphologies varied from hair-like shapes to the complete absence of the tail posterior to the hindlimbs, which fit with the stronger skeletal truncations described for *Gdf11* mutants after similar treatments (Lee et al., 2010). *T* expression in the posterior part of these embryos was mostly restricted to the ectopic ventral domain, while expression in the remaining tail tip was severely reduced (Fig. 3H). It should be noted that, although wild type embryos can be similarly truncated

upon RA exposure, they require about 10 times higher concentrations of the drug for an equivalent effect (Kessel, 1992). This indicates that *Gdf11* mutants exhibit an increased sensitivity to RA. The effects that exogenous modulation of RA signaling has on the axial progenitors of *Gdf11* mutants are consistent with the idea that the distribution of progenitors between the tail tip and the ectopic domains depends on RA signaling. Furthermore, these effects suggest that appropriate PS to CNH transition requires complete block of RA signaling in these progenitors. These results reinforce the interpretation that the truncated tail phenotypes observed in *Gdf11* mutants are, at least to some extent, the result of a failure to undergo proper PS to CNH transition.

Because the strength of the *Gdf11*$^{-/-}$ axial progenitor phenotype can be altered by exogenous modulation of RA levels, it is probable that Gdf11 signaling is required to adjust the amount of available RA at the posterior embryonic end. Considering the essential role of *Cyp26a1* in RA degradation (Abu-Abed et al., 2001; Sakai et al., 2001), a possible mechanism for RA signaling control by Gdf11 activity is to regulate the expression levels of *Cyp26a1* during the trunk to tail transition. Consistent with this, *Cyp26a1* expression levels were reduced in the posterior end of *Gdf11* mutant embryos at the time of the PS to CNH transition (Fig. 3O,P). This could be the origin of an uneven RA distribution along the AP axis, which would eventually result in different pools of progenitors being exposed to RA levels above or below a critical threshold when they are about to undergo PS to CNH relocation.

Hox genes do not play a major role in establishing the AP position of the hindlimb

The above results show that RA plays a role in *Gdf11* function controlling the PS to CNH transition. However, inhibition of RA signaling had no or only minor effects on other aspects of the *Gdf11* mutant phenotype, including the axial formula and the hindlimb position (data not shown) (Lee et al., 2010). This indicates that Gdf11 signaling controls the axial position of the trunk to tail transition and the proper formation of the CNH through different mechanisms.

The alterations in the axial formula can be explained by abnormal Hox gene expression in the paraxial mesoderm (Fig. S4) (McPherron et al., 1999; Szumska et al., 2008). It is not clear, however, how Gdf11 signaling controls the changes related to the

lateral mesoderm during trunk to tail transition that lead to the induction of structures such as the hindlimb buds. Analysis of *Hoxa9* and *Hoxc10* expression in both *Gdf11* mutant and *Cdx2P-Alk5*^{CA} transgenic embryos showed that their activation followed the altered position of the hindlimbs (Figs 2I-L and S4), suggesting that Hox genes could control AP patterning in the lateral mesoderm during the trunk to tail transition. A few mutant phenotypes including genes of the *Hox9*, *Hox10* and *Hox11* groups have been reported to include a slight posterior displacement of their hindlimbs (Favier et al., 1996; McIntyre et al., 2007), but they seem too mild to support a major role for Hox genes in this process. To understand if the absence of stronger phenotypes resulted from functional redundancies (as observed for other Hox-dependent processes) we took a gain of function approach by precociously expressing the Hox genes of these paralogs in transgenic embryos. Only transgenics expressing a gene of the *Hox9* group (*Hoxb9*) in the epiblast showed a slight anterior displacement of the hindlimbs by one segmental unit (1 somite at E10.5, which was translated into 5 instead of 6 lumbar vertebra at E18.5) (Fig. 4). However, no obvious alterations in the hindlimb position were detected when *Hoxa10, Hoxc10*, or *Hoxa11* were used in similar experiments (Table S1). Also, combined expression of different Hox genes did not change the phenotypes obtained with individual Hox genes (Table S1). Therefore, the results from both gain and loss of function approaches are not supportive of a major role of Hox genes in specifying the hindlimb position along the AP axis during trunk to tail transition.

Isl1 organizes the terminal differentiation of lateral mesoderm progenitors during trunk to tail transition

Given the relatively minor effect of Hox genes on positioning the hindlimb, we investigated other factors that could mediate hindlimb induction by Gdf11 during the trunk to tail transition. We noticed that both *Hand2* and *Shh* expression in the hindlimbs of *Cdx2P-Alk5*^{CA} transgenics was not restricted to the posterior mesenchyme, but extended into more anterior areas of the hindlimb bud (Figs 2A,B and 5A,B). *Isl1* has been shown to control a *Shh/Hand2* network associated with hindlimb induction (Itou et al., 2012). This observation, together with cell tracing studies showing that this gene is specifically activated in the lateral mesoderm associated with the hindlimb and ventral

lateral mesoderm (Yang et al., 2006), in addition to genetic experiments indicating that it is involved in early stages of hindlimb induction (Kawakami et al., 2011; Itou et al., 2012), suggest a possible role for *Isl1* in patterning the lateral mesoderm during trunk to tail transition downstream of Gdf11 signaling. To test this possibility we first expressed this gene using the *Cdx2P* enhancer in transgenic embryos (*Cdx2P-Isl1* transgenics). Although the observed phenotypes varied in intensity, these transgenics typically exhibited a more anterior position of the hindlimbs (Fig. 5C-F), which at E10.5 could reach a position up to 6 somites away from the forelimb buds. In contrast to what we observed in *Cdx2P-Alk5*^{CA} transgenics, the anteriorized position of the hindlimbs in *Cdx2P-Isl1* transgenics was associated with a truncation of the tail bud already evident at E10.5 (strong phenotypes were observed in 8 out of 15 transgenics at this stage) (Fig. 5E-H). At E18.5, this was reflected in the complete truncation after the 8th thoracic vertebra affecting both the axial skeleton and the neural tube (Fig. 5I,J,N). However, these fetuses had hindlimbs with strikingly normal skeletal morphology, which were "floating" within the soft tissue adjacent to the caudal end of the truncated axial skeleton (Fig. 5J). In addition, the digestive and excretory systems of *Cdx2P-Isl1* transgenics had an organized opening to the exterior (Fig. 5K,L), although the urethra and rectum shared a common end (Fig. 5L,M). They also had recognizable external genitalia (Fig. 5K,L) and fully developed kidneys (Fig. 5O). In contrast, we could not identify any sign of the gonads. These results indicate that the structures derived from the areas that are normally associated with *Isl1*-positive tissues (*e.g.* the most caudal parts of the lateral and of the intermediate mesoderm) were largely not affected by the precocious activation of *Isl1* in the epiblast. Areas that are normally not in contact with *Isl1* activity, however, like the paraxial mesoderm, neural tube, and more anterior areas of the intermediate mesoderm (*e.g.* those forming the gonads) were strongly affected by expression of *Isl1*.

Contrary to *Cdx2P-Isl1* transgenics, embryos expressing *Isl1* in the paraxial (*Dll1-Isl1* transgenics, n=13) or the lateral (*Hoxb6P-Isl1* transgenics, n=11) mesoderm were indistinguishable from their wild type littermates at E10.5. This indicated that, similar to Gdf11/Alk5 signaling, *Isl1* may affect mesodermal AP patterning when activated in the axial progenitors of the epiblast but not in the mesodermal tissues after their ingression through the PS. Given that *Isl1* expression is associated with the

induction of the most posterior derivatives of the lateral mesoderm, we hypothesized that this gene might trigger the terminal differentiation of the trunk progenitors. In the progenitors for the lateral mesoderm this would be associated with specific physiological programs (like those resulting in hindlimb induction), but in axial progenitors for tissues normally not in contact with *Isl1* activity, it would simply result in their depletion. To test if this could indeed be the case, we analyzed *T* expression in *Cdx2P-Isl1* transgenics at E10.5. We found that in these embryos *T* was still expressed in the notochord associated with the anterior part of the embryo. However, it was almost completely absent from the tail bud (Fig. 5G,H). This is consistent with the idea of a loss of progenitors forming neural and paraxial mesodermal structures of the tail bud. Altogether, these data support the incompatibility between *Isl1* expression and the maintenance of axial progenitors and suggest a developmental role for *Isl1* in the programmed termination of the lateral mesoderm progenitors as part of the trunk to tail transition.

The observation that *Isl1* and Gdf11 signaling are both required in the axial progenitors to modulate AP patterning of the lateral mesoderm led us to explore if *Isl1* is a direct target of Gdf11/Alk5 signaling. Kang et al. (2009) have recently characterized enhancer elements involved in the activation the *Isl1* gene in the cardiac progenitors and in the posterior part of the embryo. We found several putative Smad2 binding sites within one of the most conserved regions of this enhancer (CR2 in Kang et al., 2009) (Fig. 6A,B), suggesting that *Isl1* could be a target of the Gdf11 pathway. In transgenic embryos, CR2 was able to drive expression of a reporter gene specifically in the caudal end of the lateral mesoderm (Fig. 6D), thus mimicking the normal expression domain of *Isl1* in this area (Fig. 6C) (Yang et al., 2006). Inactivation of all potential Smad sites in this enhancer rendered it inactive (Fig. 6E), indicating that they are required for enhancer activity. Taken together, our results identify *Isl1* as a direct physiological target of *Gdf11* in its activity to modulate the trunk to tail transition during mouse axial elongation.

DISCUSSION

In this work, we have shown that *Gdf11* is a central modulator of the processes involved in the trunk to tail transition in the mouse embryo. This is supported by both loss and gain of function experiments. In *Gdf11* mutant embryos the trunk to tail transition (which can

be conveniently identified by the position of the hindlimb and cloaca-related tissues) was posteriorly displaced, leading to the formation of a longer trunk. Conversely, precocious activation of Gdf11 signaling using a constitutively activated form of its receptor Alk5 produced a strong anterior displacement in the hindlimb position, which resulted in dramatically shortened trunks. It should be noted that although delayed, the trunk to tail transition still occurs in *Gdf11* mutant embryos. One possible explanation is that Gdf11 activity is partially compensated by other molecules that activate the same signaling pathway. A candidate for such molecule is *Gdf8* (*Myostatin*) as inactivation of this gene intensifies the *Gdf11* mutant phenotype in the axial skeleton (McPherron et al., 2009). An analysis of the trunk to tail transition in *Gdf11/Gdf8* double mutants has not been reported. However, the longer rib cages observed in these embryos, together with the more anterior axial truncation at the lumbar level, and the presence of strongly reduced hindlimbs (McPherron et al., 2009) are compatible with a largely incomplete or absent trunk to tail transition. Alternatively (or in addition), other signaling pathways can act in parallel during this process, protecting *Gdf11* mutant embryos from a complete block in the switch from making trunk to tail tissues.

The hindlimb and ventral lateral mesoderm as a product of terminal differentiation of the lateral mesoderm progenitors

During the trunk to tail transition the axial progenitors relocate from a position in the PS and adjacent epiblast to the CNH (Cambray and Wilson, 2002; 2007; Wilson and Beddington, 1996). This relocation does not include all progenitors. In particular, those for the lateral and intermediate mesoderm, involved in the genesis of the trunk associated organs, are not incorporated into the CNH. Instead, specific differentiation programs are activated in these progenitors to generate the hindlimbs and the ventral lateral mesoderm, which interacts with the hindgut endoderm to organize the posterior end of several trunk associated organ systems. Indeed, even in some snakes, a small hindlimb primordium is produced in this position that later fails to produce a full grown member (Cohn and Tickle, 1999). Gdf11 signaling seems to play a role in this process through a mechanism that includes activation of *Isl1* in the progenitors for the lateral mesoderm. This is in agreement with lineage tracing experiments showing that in wild type embryos, *Isl1*

becomes specifically activated in the progenitors of the hindlimb and ventral lateral mesoderm (Yang et al., 2006). It is also consistent with genetic experiments showing that hindlimbs are not formed in the absence of this gene (Kawakami et al., 2011; Itou et al., 2012). In addition, we showed here that precocious activation of *Isl1* in axial progenitors of the epiblast was able to induce the hindlimbs and cloacal tissues at more anterior axial levels, thus mimicking to some extent the *Cdx2P-Alk5*^{CA} phenotypes (see below). Importantly, a conserved enhancer for the *Isl1* gene that activates expression in the most caudal part of the lateral mesoderm, contains several Smad binding sites that are essential for its activity, thus establishing a direct connection between Gdf11 signaling and *Isl1* activation. In this context, it should be noted that activation of this enhancer requires other factors in addition to Gdf11 signaling. Indeed, this regulatory element is inactive in the progenitors for the neural tube or paraxial mesoderm, although Gdf11 signaling is active in this area. *Fox* genes are among the best candidates to cooperate with Gdf11 signaling in activating this enhancer because it also contains Forkhead binding sites that are essential for enhancer activity (Kang et al., 2009). *FoxF1* is one of the prime candidates to play a physiological role in this process for its expression is detected in the lateral mesoderm but not in the neural tube and paraxial mesoderm (Mahlapuu et al., 2001).

One of the most striking characteristics of the *Cdx2P-Isl1* transgenics was the totally different effects that *Isl1* expression had on the various axial progenitors. In the progenitors of the lateral mesoderm, precocious *Isl1* activation had surprisingly little effect on the morphogenesis of the posterior lateral mesoderm derivatives, other than their induction at a more anterior axial level. However, *Isl1* activation had strong deleterious effects on the progenitors of more medial tissues, like the notochord, the neural tube, and paraxial mesoderm, which normally do not express *Isl1*. Therefore, the phenotype that we observed in the *Cdx2P-Isl1* transgenics might indicate that *Isl1* activity has negative effects on progenitor maintenance, bringing them into terminal differentiation pathways. In the progenitors of the lateral mesoderm, the cessation of progenitor renewal is combined with activation of the genetic programs resulting in the formation of structures like the hindlimb or the ventral lateral mesoderm. From this perspective, the hindlimb and cloacal tissues could represent the product of terminal

differentiation of the progenitors for the lateral mesoderm associated with the trunk to tail transition. In *Cdx2P-Isl1* transgenics, most axial progenitors are prematurely exposed to *Isl1*. In the progenitors for the lateral mesoderm, this triggered the physiological program at an earlier developmental stage. However, activation of *Isl1* in the precursors of neural tube and paraxial mesoderm led to a block in progenitor maintenance that was not associated with an organized differentiation program, thus producing the morphological truncation of axial structures.

It should be noted that we never found *Cdx2P-Isl1* transgenics with hindlimbs closer than 6 somites to the forelimb buds or with axial truncations anterior to the 8th thoracic segment, indicating that the competence of the axial progenitors to respond to *Isl1* is not uniform along the AP axis. Considering that *Alk5* can induce hindlimb buds at more anterior levels than *Isl1* when prematurely activated in the epiblast, it is probable that the competence of the axial progenitors to respond to *Isl1* is also provided by Gdf11. Whether this is indeed the case as well as the mechanisms mediating this gain of competence remains to be determined.

Intriguingly, the skeletal phenotype that we observed in *Cdx2P-Isl1* transgenics is remarkably similar to the clinical characteristics found in patients with severe cases of spinal segmental dysgenesis (Mahomed and Naidoo, 2009), which raises the possibility that deregulation of *Isl1* expression during trunk to tail transition could be in the origin of this human syndrome.

Setting the PS to CNH transition

Another of the major processes associated with the trunk to tail transition is the relocation of the N-M progenitors from the anterior PS and adjacent epiblast to the CNH to form the tail bud (Cambray and Wilson, 2002; 2007; Wilson and Beddington, 1996). Our results indicate that Gdf11 signaling is also involved in this process and that this activity is mediated by modulation of RA availability at the posterior embryonic end. In addition, our data suggest that proper PS to CNH transition requires a complete block of RA signaling because its pharmacological inhibition produced a significant recovery of the PS to CNH reorganization in *Gdf11*$^{-/-}$ embryos. This is consistent with the phenotype of *Cyp26a1* mutant embryos (Abu-Abed et al., 2001; 2003; Sakai et al., 2001). Indeed, it has

been shown that in the absence of this RA-catabolyzing enzyme, embryos are exposed to an excess of RA that produces axial truncations at the lumbo-sacral level, which coincides with the stage when the PS to tail bud transition is taking place. The expression patterns reported for markers like *T* or *Cdx4* in *Cyp26a1* mutant embryos are compatible with strong alterations in the PS to tail bud transition (Abu-Abed et al., 2003). Our data also suggest that Gdf11 signaling modulates RA availability by regulating *Cyp26a1* expression. Accordingly, *Cyp26a1* levels were lower in *Gdf11* mutants than in wild type embryos during trunk to tail transition. Interestingly, the observation that *Cyp26a1* expression was reduced but not completely inactivated in *Gdf11* mutants at this developmental stage may explain the segregation of the axial progenitors into several domains. In particular, progenitors closer to the tail tip would be surrounded by sufficient *Cyp26a1* to protect them from RA. However, the levels of *Cyp26a1* in more anterior areas would fall below the threshold level required for effective RA clearance, leaving progenitors in this area exposed to RA. A reduction in *Cyp26a1* expression in the tail of *Gdf11* mutants has been previously reported at later developmental stages, associated with other developmental processes (Lee et al., 2010), further reinforcing the connection between Gdf11 signaling and the RA catabolic pathway.

The apparent separation between RA-responding and RA-non-responding progenitors observed in *Gdf11* mutants suggest that the PS to CNH transition might require activation of stage-specific characteristics in the axial progenitors (e.g. adhesion properties) that would target them to specific regions (a progenitor niche?) of the posterior embryonic end, eventually generating a tail-bud primordium that organizes posterior embryonic growth. According to this hypothesis, acquisition of those properties would require complete down regulation of RA signaling in these progenitors. Activated RA signaling during the PS to CNH transition would impair colonization of the tail bud primordium niche. When the majority of progenitors respond to RA (like *Cyp26a1* mutants, *Gdf11* mutants treated with low doses of RA, or wild type embryos treated with high RA doses), the tail bud does not form and severe axial truncations occur at the level of the trunk to tail transition (Abu-Abed et al., 2001; 2003; Kessel, 1992; Sakai et al., 2001; Lee et al., 2010).

EXPERIMENTAL PROCEDURES

Transgenic constructs, mice and embryos

The *Gdf11* mutant strain used in this work has been described previously (McPherron et al., 1999). The constructs for the production of transgenic embryos were generated using standard molecular cloning techniques. The enhancers used for these constructs were a 9.5 kb fragment upstream of the *Cdx2* gene (*Cdx2P*) (Benahmed et al., 2008), the msd enhancer of the *Dll1* gene (Beckers et al., 2000), and the lateral mesoderm enhancer of the *Hoxb6* gene (Becker et al., 1996). The *Isl1* CR2 enhancer (Kang et al., 2009) was amplified by PCR from mouse genomic DNA using primers 5'-TCCTCACACTGGTCTAACCAG-3' and 5'-GGACATCCCCACCCAGCGCTG-3'. To produce an enhancer without Smad binding sites, the different Smad targets were modified to CACA, except for the palindromic target GTCTAGAC that was changed to CATGCAGG. All these modifications were performed using a PCR-based mutagenesis strategy and verified by direct sequencing. The wild type and mutant *Isl1* enhancers were cloned upstream of the adenovirus2 minimal late promoter and the resulting regulatory elements were inserted upstream the *β-galactosidase* cDNA. The *Isl1* cDNA was IMAGE clone 40130540. To produce the $Alk5^{CA}$ cDNA, we used IMAGE clone 7098473, corresponding to the rat gene, and changed the threonine 204 for an aspartic acid (Wieser et al. 1995) using a PCR-based mutagenesis strategy. The mutation was confirmed by direct sequencing of the cDNA clones. The *Cdx2P-creER*^{T} construct contained a tamoxifen-inducible cre recombinase (Hayashi and McMahon, 2002). All transgenic constructs contained the SV40 polyadenylation signal in addition to the regulatory regions and relevant cDNAs.

Transgenic embryos were generated by pronuclear injection of the relevant constructs according to standard methods (Hogan et al., 1994). *Gdf11* mutant embryos were obtained from $Gdf11^{+/-}$ intercrosses. The day that plugs were found was considered E0.5. In the case of transgenic embryos, E0.5 was the day after the transfer of injected oocytes. The activity of the *Cdx2P* enhancer was estimated by crossing *Cdx2P-creER*^{T} transgenics with the *ROSA26R* reporter line (Soriano, 1999) and pregnant females were treated with 4 mg of tamoxifen/20 g of body weight, dissolved in corn oil by

intraperitoneal injection. Embryos were collected from pregnant females by cesarean section and fixed with 4% paraformaldehyde (PFA) in PBS for *in situ* studies or with Mirsky's fixative (National Diagnostics) for β-galactosidase staining.

Treatment with RA and RA inhibitor were performed as in Lee et al., (2010) with slight modifications. Briefly, the stock solution of RA inhibitor AGN193109 (1 mg/ml in DMSO) was dissolved in corn oil and administered to pregnant females in three doses of 2 mg/kg of body weight between E7.5 and E9.5. For RA treatments, a 25 mg/ml solution of all-trans RA in DMSO was diluted in corn oil and was administered at E8.5 by oral gavage at a final concentration of 10 mg/kg of body weight.

Phenotypic analyses and statistics

Comparison of hindlimb development between wild type and *Gdf11* mutant embryos was performed using the morphometric system developed by Boehm et al. (2011). Results were presented as mean ± SEM and compared using the Student's t test ($p<0.05$ was considered significant). To see the external morphology of midgestation embryos in greater detail, they were stained in hydrochloric carmine using a modified protocol from Machado-Silva et al. (1998) (see supplementary information for details). *In situ* hybridization on whole embryos was performed using DIG-labeled probes as previously described (Kanzler et al., 1998). Skeletal analyses were performed using the Alcian blue/alizarin red staining method as previously described (Mallo and Brändlin, 1997). For histological analyses, embryos were fixed in Bouin's fixative and embedded in paraffin. 10 μm thick sections were then stained with haematoxylin/eosin using standard histological methods. Identification of β-galactosidase activity was performed by X-gal staining according to Carvajal et al. (2001).

Acknowledgements

We would like to thank Alexandra McPherron and Se-Jin Lee for providing the *Gdf11* mutant strain, José Belo, Jacqueline Deschamps, Denis Duboule, Achim Gossler, Bernhard Herrmann, Andreas Kispert, Malcolm Logan, Andrew McMahon and Erik Olson for sending plasmids containing regulatory elements and probes for *in situ* hybridization, Deneen Wellik for sharing unpublished data and Elio Sucena, Ines

Domingues and Jennifer Rowland for reading the manuscript. This work was supported by grants PTDC/BIA-BCM/110638/2009 and PTDC/SAU-BID/110640/2009 to M. M. and by PhD fellowships SFRH/BD/33562/2008 to A. D. J., SFRH/BD/51876/2012 to R. A. and SFRH/BD/51879/2012 to I. V.-L.

REFERENCES

Abu-Abed, S., Dollé, P., Metzger, D., Beckett, B., Chambon, P. and Petkovich, M. (2001). The retinoic acid-metabolizing enzyme, *CYP26A1*1, is essential for normal hindbrain patterning, vertebral identity, and development of posterior structures. Genes Dev. *15,* 226-240.

Abu-Abed, S., Dollé, P., Metzger, D., Wood, C., MacLean, G., Chambon, P. and Petkovich, M. (2003). Developing with lethal RA levels: genetic ablation of Rarg can restore the viability of mice lacking *Cyp26a1*1. Development *130,* 1449-1459.

Andersson, O., Reissmann, E. and Ibáñez, C. F. (2006). Growth differentiation factor 11 signals through the transforming growth factor-beta receptor ALK5 to regionalize the anterior-posterior axis. EMBO Rep. *7,* 831-837.

Becker, D., Jiang, Z., Knödler, P., Deinard, A. S., Eid, R., Kidd, K. K., Shashikant, C. S., Ruddle, F. H. and Schughart, K. (1996). Conserved regulatory element involved in the early onset of Hoxb6 gene expression. Dev. Dyn. *205,* 73-81.

Beckers, J., Caron, A., Hrabe de Angelis, M., Hans, S., Campos-Ortega, J. A. and Gossler, A. (2000). Distinct regulatory elements direct delta1 expression in the nervous system and paraxial mesoderm of transgenic mice. Mech. Dev. *95,* 23-34.

Benahmed, F. Gross, I., Gaunt, S.J., Beck, F., Jehan, F., Domon-Dell, C., Martin, E., Kedinger, M., Freund, J.N., and Duluc, I. (2008). Multiple regulatory regions control the complex expression pattern of the mouse *Cdx2* homeobox gene. Gastroenterology *4,* 1238-1247.

Boehm, B., Rautschka, M., Quintana, L., Raspopovic, J., Jan, Z. and Sharpe, J. (2011). A landmark-free morphometric staging system for the mouse limb bud. Development *138,*1227-1234.

Cambray, N., and Wilson, V. (2002). Axial progenitors with extensive potency are localised to the mouse chordoneural hinge. Development *129,* 4855-4866.

Cambray, N., and Wilson, V. (2007). Two distinct sources for a population of maturing axial progenitors. Development *134,* 2829-2840.

Carapuço, M., Nóvoa, A., Bobola, N. and Mallo M. (2005). Hox genes specify vertebral types in the presomitic mesoderm. Genes Dev. *19,* 2116-2121.

Carlson, B. M. (1999). Human embryology and developmental biology, 2nd ed. Mosby, Inc. St. Louis.

Carvajal, J. J., Cox, D, Summerbell, D. and Rigby, P. W. J. (2001). A BAC transgenic analysis of the Mrf4/Myf5 locus reveals interdigitated elements that control activation and maintenance of gene expression during muscle development. Development *128,* 1857-1868.

Cohn, M. J. and Tickle, C. (1999). Developmental basis of limblessness and axial patterning in snakes. Nature *399,* 474-479

Essalmani, R., Zaid, A., Marcinkiewicz, J., Chamberland, A., Pasquato, A., Seidah, N. G. and Prat, A. (2008). In vivo functions of the proprotein convertase PC5/6 during mouse development: Gdf11 is a likely substrate. Proc. Natl. Acad. Sci. U S A *105,* 5750-5755.

Favier, B., Rijli, F. M., Fromental-Ramain, C., Fraulob, V., Chambon, P. and Dollé, P. (1996). Functional cooperation between the non-paralogous genes Hoxa-10 and Hoxd-11 in the developing forelimb and axial skeleton. Development *122,* 449-460.

Gaunt, S. J., Drage, D. and Trubshaw, R. C. (2005). cdx4/lacZ and *Cdx2*/lacZ protein gradients formed by decay during gastrulation in the mouse. Int. J. Dev. Biol. *49,* 901-908.

Gibson-Brown, J. J., Agulnik, S. I., Chapman, D. L., Alexiou, M., Garvey, N., Silver, L. M. and Papaioannou, V. E. (1996). Evidence of a role for T-box genes in the evolution of limb morphogenesis and the specification of forelimb/hindlimb identity. Mech. Dev. *56,* 93-101.

Hayashi, S. and McMahon, A. P. (2002). Efficient recombination in diverse tissues by a tamoxifen-inducible form of Cre: tool for temporally regulated gene activation/inactivation in the mouse. Dev. Biol. *244,* 305-318.

Ho, D. M., Yeo, C. Y. and Whitman, M. (2010). The role and regulation of GDF11 in Smad2 activation during tailbud formation in the Xenopus embryo. Mech. Dev. *127,* 485-495.

Hogan, B., Beddington, R., Constantini, F. and Lacy, E. (1994). Manipulating The Mouse Embryo: A Laboratory Manual. Cold Spring Harbor Laboratory Press, Cold Spring Harbor.

Iimura, T. and Pourquié, O. (2006). Collinear activation of Hoxb genes during gastrulation is linked to mesoderm cell ingression. Nature *442,* 568-571.

Itou. J., Kawakami, H., Quach, T., Osterwalder, M., Evans, S. M., Zeller, R. and Kawakami, Y. (2012). Islet1 regulates establishment of the posterior hindlimb field upstream of the *Hand2-Shh* morphoregulatory gene network in mouse embryos. Development *139,* 1620-1629.

Kang, J., Nathan, E., Xu, S. M., Tzahor, E. and Black, B. L. (2009). *Isl1* is a direct transcriptional target of Forkhead transcription factors in second-heart-field-derived mesoderm. Dev. Biol. *334,* 513-522.

Kanki, J. P. and Ho, R. K. (1997). The development of the posterior body in zebrafish. Development *124,* 881-893.

Kawakami, Y., Marti, M., Kawakami. H., Itou, J., Quach, T., Johnson, A., Sahara, S., O'Leary, D. D., Nakagawa, Y., Lewandoski, M., Pfaff, S., Evans, S. M., and Izpisua-Belmonte, J. C. (2011). Islet1-mediated activation of the of the Islet1-mediated activatior hindlimb initiation in mice. Development *138,* 4465-4473.

Kessel, M. (1992). Respecification of vertebral identities by retinoic acid. Development *115,* 487-501.

Lee, Y. J., McPherron, A., Choe, S., Sakai, Y., Chandraratna, R. A, Lee, S. J. and Oh, S. P. (2010). Growth differentiation factor 11 signaling controls retinoic acid activity for axial vertebral development. Dev. Biol. *347,* 195-203.

Liu, J.-P. (2006). The function of growth/differentiation factor 11 (Gdf11) in rostrocaudal patterning of the developing spinal cord. Development *133,* 2865-2874.

Machado-Silva, J. R., Pelajo-Machado, M., Lenzi, H. L. and Gomes, D. C. (1998). Morphological study of adult male worms of *Schistosoma mansoni* Sambon, 1907,

by confocal laser scanning microscopy. Mem. Inst. Oswaldo Cruz *93 (Suppl 1)*, 303-307.

Mahlapuu, M., Ormestad, M., Enerbäck, S., and Carlsson, P. (2001). The forkhead transcription factor Foxf1 is required for differentiation of extra-embryonic and lateral plate mesoderm. Development *128,* 155-166.

Mahomed, N and Naidoo, J. (2009). Spinal segmental dysgenesis. South African J. Radiol. *13,* 29-32.

Mallo, M. and Brändlin, I. (1997). Segmental identity can change independently in the hindbrain and rhombencephalic neural crest. Dev. Dyn. *210,* 146-156.

Mallo, M., Vinagre, T., Carapuço, M. (2009). The road to the vertebral formula. Int. J. Dev. Biol. *53,* 1469-1481.

Mallo, M., Wellik, D. M. and Deschamps, J. (2010). *Hox Genes* and Regional Patterning of the Vertebrate Body Plan. Dev. Biol. *344,* 7-15.

Martin, B. L. and Kimelman, D. (2012). Canonical Wnt signaling dynamically controls multiple stem cell fate decisions during vertebrate body formation. Dev. Cell *22,* 223-232.

McIntyre, D. C., Rakshit, S., Yallowitz, A. R., Loken, L., Jeannotte, L., Capecchi, M. R. and Wellik, D. M. (2007). Hox patterning of the vertebrate rib cage. Development *134,* 2981-2989.

McPherron, A.C., Huynh, T.V. and Lee, S.J. (2009). Redundancy of myostatin and growth/differentiation factor 11 function. BMC Dev. Biol. *9,* 24.

McPherron, A.C., Lawler, A.M. and Lee, S.J. (1999). Regulation of anterior/posterior patterning of the axial skeleton by growth/differentiation factor 11. Nat. Genet. *22,* 260-264.

Oh, S.P., Yeo, C.Y., Lee, Y., Schrewe, H., Whitman, M. and Li, E. (2002). Activin type IIA and IIB receptors mediate Gdf11 signaling in axial vertebral patterning. Genes Dev. *16,* 2749-2754.

Psychoyos, D. and Stern, C. D. (1996). Fates and migratory routes of primitive streak cells in the chick embryo. Development *122,* 1523-1534.

Sakai, Y., Meno, C., Fujii, H., Nishino, J., Shiratori, H., Saijoh, Y., Rossant, J. and Hamada, H. (2001). The retinoic acid-inactivating enzyme CYP26 is essential for

establishing an uneven distribution of retinoic acid along the anterio-posterior axis within the mouse embryo. Genes Dev. *15,* 213-225.

Schoenwolf, G. C. (1977). Tail (end) bud contributions to the posterior region of the chick embryo. J. Exp. Zool. *210,* 227-246.

Soriano, P. (1999). Generalized lacZ expression with the ROSA26 Cre reporter strain. Nature Genet. *21,* 70-71.

Suzuki, K., Economides, A., Yanagita, M., Graf, D. and Yamada, G. (2009). New horizons at the caudal embryos: coordinated urogenital/reproductive organ formation by growth factor signaling. Curr. Opin. Genet. Dev. *19,* 491-496.

Stern, C. D., Charité, J., Deschamps, J., Duboule, D., Durston, A. J., Kmita, M., Nicolas, J. F., Palmeirim, I., Smith, J. C. and Wolpert, L. (2006). Head-tail patterning of the vertebrate embryo: one, two or many unresolved problems? Int. J. Dev. Biol. *50,* 3-15.

Szumska, D., Pieles, G., Essalmani, R., Bilski, M., Mesnard, D., et al., (2008). VACTERL/caudal regression/Currarino syndrome-like malformations in mice with mutation in the proprotein convertase *Pcsk5*. Genes Dev. *22,* 1465-1477.

Takemoto, T., Uchikawa, M., Yoshida, M., Bell, D. M., Lovell-Badge, R. et al. (2011). Tbx6-dependent Sox2 regulation determines neural or mesodermal fate in axial stem cells. Nature *470,* 394-398.

Tam, P. P. L. and Beddington, R. S. P. (1987). The formation of mesodermal tissues in the mouse embryo during gastrulation and early organogenesis. Development *99,* 109-126.

Vinagre, T., Moncaut, N., Carapuço, M., Nóvoa, A., Bom, J. and Mallo, M. (2010). Evidence for a myotomal Hox/Myf cascade governing non-autonomous control of rib specification within global vertebral domains. Dev. Cell *18,* 655-661.

Wellik, D.M. (2007). Hox patterning of the vertebrate axial skeleton. Dev. Dyn. *236,* 2454-2463.

Wellik, D.M. and Capecchi, M.R. (2003). Hox10 and Hox11 genes are required to globally pattern the mammalian skeleton. Science *301,* 363-367.

Wieser, R., Wrana, J. L. and Massagué, J. (1995). GS domain mutations that constitutively activate TβR-I, the downstream signaling component in the TGF-β receptor complex. EMBO J. *14,* 2199-2208.

Wilson, V. and Beddington, R. S. (1996). Cell fate and morphogenetic movement in the late mouse primitive streak. Mech. Dev. *55,* 79-89.

Wilson, V., Olivera-Martinez, I. and Storey, K. G. (2009). Stem cells, signals and vertebrate body axis extension. Development *136,* 1591-1604.

Yang, L., Cai, C. L., Lin, L., Qyang, Y., Chung, C., Monteiro, R. M., Mummery, C. L., Fishman, G. I., Cogen, A. and Evans, S. (2006). *Isl1*Cre reveals a common Bmp pathway in heart and limb development. Development *133,* 1575-1585.

FIGURE LEGENDS

Figure 1. Posterior displacement of the trunk to tail transition in *Gdf11* mutant embryos. Different aspects of the trunk to tail transition were compared between wild type (A,D,F,H,J,L,N) or *Gdf11*$^{-/-}$ (B, E, G, I, K, M, O) embryos. A, B. Gross morphology of wild type and *Gdf11* mutant embryos at E11.5. The smaller size of the hindlimb is evident in the mutants. The size (in somite units) of the interlimb area is indicated. C. Estimation of the embryonic age of E10.5 and E11.5 wild type and *Gdf11*$^{-/-}$ embryos according to the size of the hindlimbs. Results are shown as the mean ± SEM. ***, P<0.0001. D,E. Estimation of the position of hindlimb induction (evidenced by *Tbx4*, arrows) with respect to the somite number (evidenced by *Uncx4.1*). F,G. Endodermal component of the cloaca in E11.5 embryos, labeled by *Shh* (arrow). H,I. Cloacal/urethral epithelium in E11.5 embryos, revealed by *Fgf8* (arrow). *Gdf11* mutant embryos exhibited increased expression of *Fgf8* in the tail bud (arrowhead). J,K. Identification of the mesodermal component of the developing cloaca at E10.5 by *Isl1* expression (arrow). The asterisk indicates the position of the hindlimb. L,M. Extended formation of intermediate mesoderm, identified by *Pax2*, until the posterior part of the hindlimb (asterisk) in E10.5 embryos (indicated by the arrows). N,O. Identification of the visceral lateral mesoderm by *Wnt2* expression. The brackets show the expression area close to the hindlimb.

Figure 2. Anteriorization of the trunk to tail transition in *Cdx2P-Alk5*^{CA} transgenic embryos. Analysis of different aspects of AP patterning in E10.5 wild type (A,C,E, G,I,K) and *Cdx2P-Alk5*^{CA} (B,D,F,H,J,L) embryos. A,B. Labeling of the lateral mesoderm and hindlimbs with *Hand2*. .C,D. Labeling of the visceral lateral mesoderm (arrow) with *Wnt2*. E,F. Labeling of the mesodermal component of the cloaca (arrow) with *Isl1*. G,H. Labeling of the endodermal component of the cloaca (arrow) with *Shh*. I,J. Expression of *Hoxa9*. Arrows mark the anterior limit of expression in the neural tube. K,L. Expression of *Hoxc10*. Arrows mark the anterior limit of expression and the red arrowhead indicates ectopic expression in the neural tube of the transgenic embryo. In all panels the position

of the hindlimb is indicated with an asterisk except for panel H, where it is indicated with a bracket.

Figure 3. Abnormal posterior growth zone in *Gdf11* mutant embryos. Posterior growth zone was analyzed in wild type (A,C,E,I,K,M,O) and *Gdf11* mutant (B,D,F,G,H, J,L,N,P) embryos. *T* expression was analyzed at E9.5 (A,B), E10.5 (C,D,G,H), and E11.5 (E,F). The arrows indicate the extended anterior expression through the ventral part of the tail. The arrowhead in F indicates the tip of the tail. *Cdx2* (I,J), *Fgf8* (K,L), and *Wnt3a* (M,N) expression was analyzed at E10.5. The arrows indicate the extended anterior expression through the ventral part of the tail. The arrowheads in K and L indicate the tail bud tip, with upregulation of *Fgf8* in the *Gdf11* mutant. G. Effect of treatment of *Gdf11* mutants with the RA inhibitor AGN193109 during the trunk to tail transition on the progenitors at E10.5, evaluated by expression of *T*. H. Effect of treatment of *Gdf11* mutants with RA during the trunk to tail transition on the progenitors at E11.5 evaluated by expression of *T*. The arrow indicates the ventral ectopic domain and the arrowhead the position of the tail tip. O,P. Comparison of *Cyp26a1* expression in wild type (O) and *Gdf11* mutant (P) embryos at equivalent relevant stages of the trunk to tail transition (21 somites for wild type, 27 somites for $Gdf11^{-/-}$ embryos).

Figure 4. Effect of *Hoxb9* on the trunk to tail transition. A,B. The position of the hindlimb was analyzed in E10.5 wild type (A) and *Cdx2P-Hoxb9* (B) embryos, labeling the somites with *Uncx4.1* and the hindlimb with *Tbx4*. C,D. Skeletal analysis of wild type (C) and *Cdx2P-Hoxb9* (D) fetuses at E18.5. Indicated are the number of the last rib-containing vertebra (T13), the number of lumbar vertebra and the position of the first sacra vertebra (arrow).

Figure 5. The role of *Isl1* in the trunk to tail transition. A, B. *Shh* expression in the hindlimb buds of E10.5 wild type (A) and $Cdx2P\text{-}Alk5^{CA}$ (B) transgenic embryos. Expression in the posterior part of the wild type hindlimb (arrow) and along the whole AP extension of the distal part of the transgenic hindlimb (line) is indicated. C,D External morphology of wild type (C) and *Cdx2P-Isl1* transgenics (D) at E18.5. E-H. Truncated

phenotype of *Cdx2P-Isl1* transgenic embryos at E10.5. E,F. Staining with *Uncx4.1* (somites) and *Tbx4* (hindlimb) to show the anteriorization of the hindlimb bud of *Cdx2P-Isl1* transgenic embryos (F) (8 somites from the forelimb bud in this embryo), when compared to wild type littermates (E). G,H. In situ hybridization with *T*. Expression in the notochord (N) is observed in both wild type (G) *Cdx2P-Isl1* transgenic (H) embryos. However, expression in the tail bud (arrowheads) is mostly absent from the *Cdx2P-Isl1* transgenic embryo. The arrow in H indicates the ectopic end of the T expression domain next to the hindlimb (indicated with a bracket), which in this embryo is located 6 somites posterior to the forelimb bud. I,J. Skeletal staining of of wild type (I) and *Cdx2P-Isl1* transgenics (J) at E18.5. K-O. Sagittal sections of E18.5 wild type (K) and *Cdx2P-Isl1* transgenics (I-O) showing: K, the external genitalia (G), together with the independent uretra (UT) and rectum (R) in wild type embryos; L, the external genitalia (G) and a combined rectum/urethra (R/UT) in *Cdx2P-Isl1* transgenics; M, the convergence of the urethra (UT) and rectum (R) into a single distal tube (arrow) in the transgenics; N, the truncation in the neural tube (NT) in the transgenics; O, the presence of kidneys in the transgenics. UR: ureter; BL: urinary bladder.

Figure 6. *Isl1* expression requires Smad activity. A. Sequence of the CR2 enhancer of the *Isl1* gene. The Fox binding sites are highlighted in green and the Smad binding sites in red and in orange (the palindromic site). B. Schematic representation of the reporter constructs for the *Isl1-CR2* enhancer. The Fox and Smad binding sites are represented by green diamonds and blue circles, respectively. In the mutant constructs, the Smad binding sites were mutated. C. *Isl1* expression in the posterior part of the embryo shortly after the trunk to tail transition. D. β-galactosidase expression in *Isl1-βgal* transgenics in E9.25 embryos. E. Absent β-galactosidase expression in *Isl1-βgal-ΔS* transgenics in E9.25 embryos. Numbers of positive cases in relation to the total number of harvested embryos is indicated between brackets.

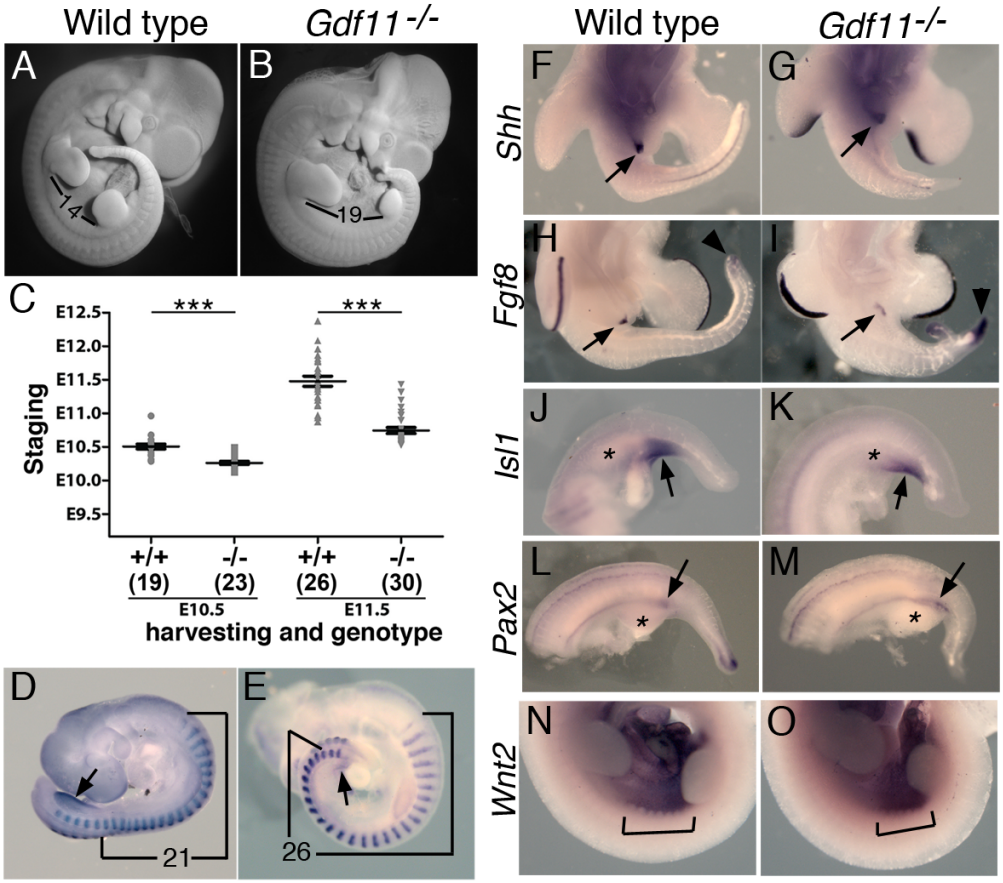
Wild type
Gdf11 -/-
A
B
14
19
C
E12.5
E12.0
E11.5
E11.0
E10.5
E10.0
E9.5
Staging
***
***
+/+ (19)
-/- (23)
+/+ (26)
-/- (30)
E10.5
E11.5
harvesting and genotype
D
E
21
26
Wild type
Gdf11-/-
F
G
H
I
J
K
L
M
N
O
Shh
Fgf8
Isl1
Pax2
Wnt2

Figure 1

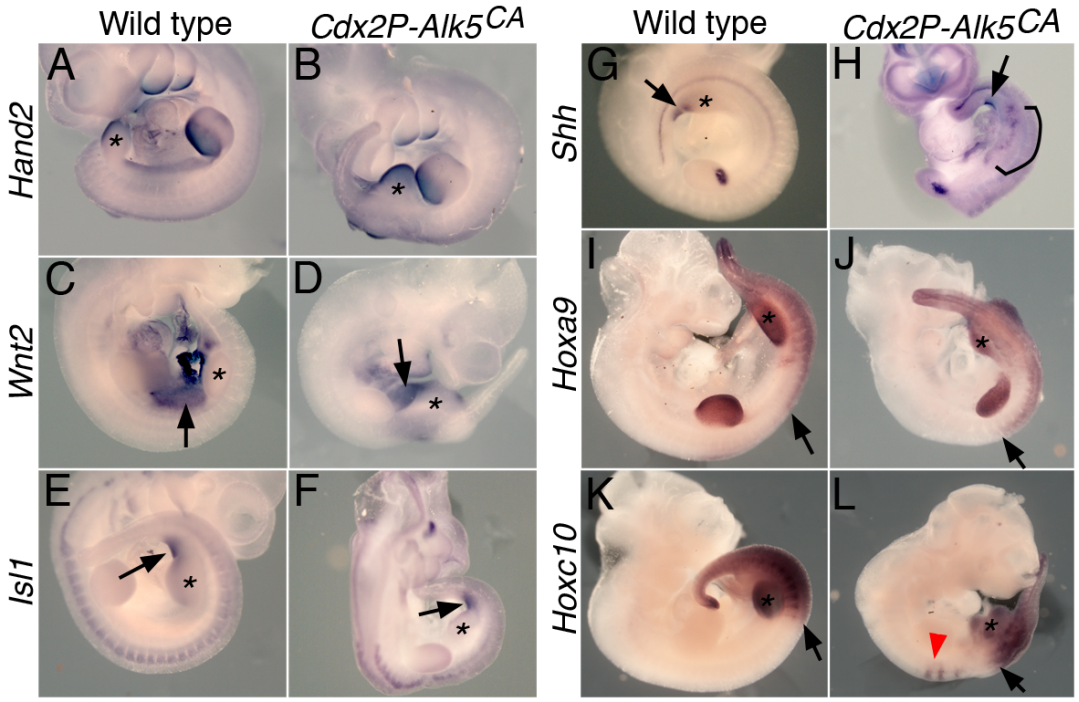
Wild type
Cdx2P-Alk5CA
Wild type
Cdx2P-Alk5CA
Hand2
Wnt2
Isl1
Shh
Hoxa9
Hoxc10
A
B
C
D
E
F
G
H
I
J
K
L

Figure 2

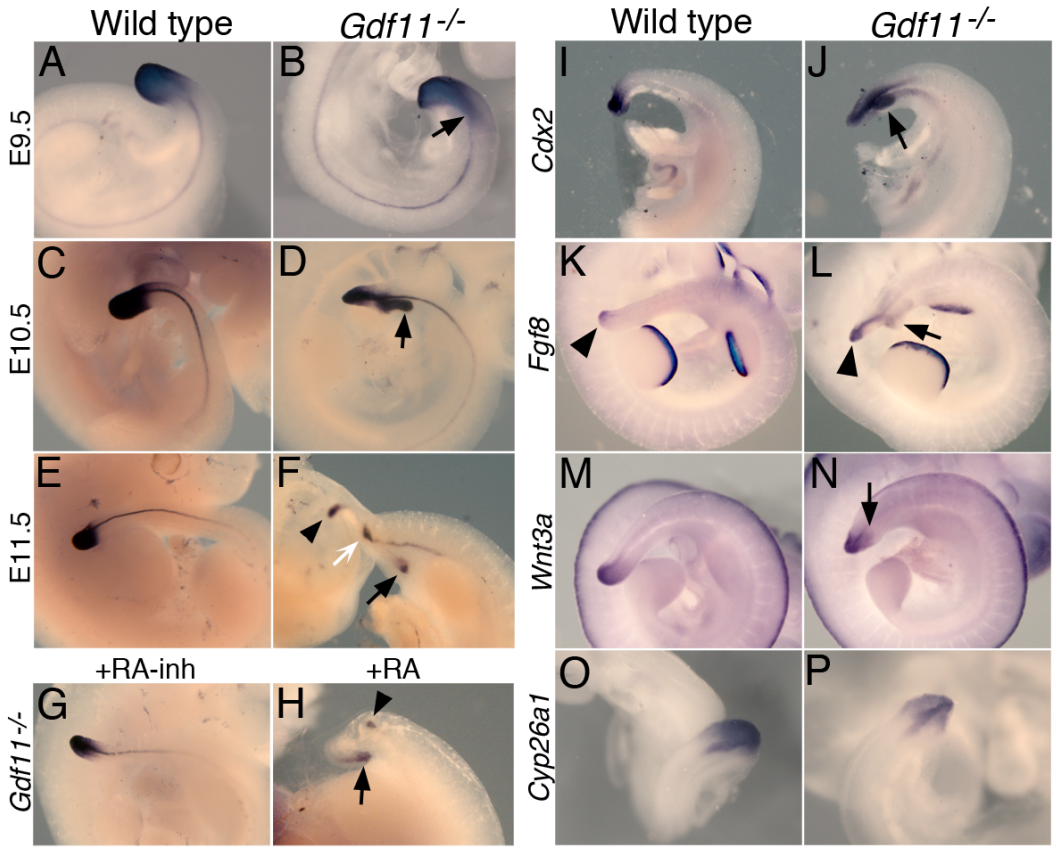
Wild type
Gdf11 -/-
Wild type
Gdf11 -/-
E9.5
E10.5
E11.5
Cdx2
Fgf8
Wnt3a
Cyp26a1
A
B
C
D
E
F
G
H
I
J
K
L
M
N
O
P
+RA-inh
+RA
Gdf11 -/-

Figure 3

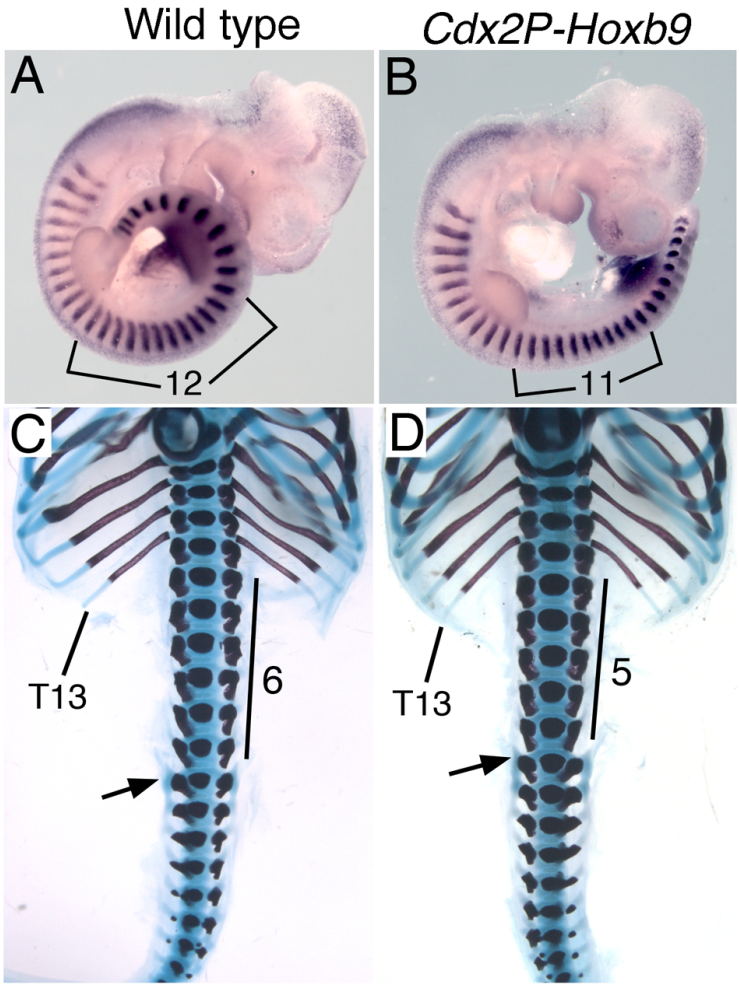

Figure 4

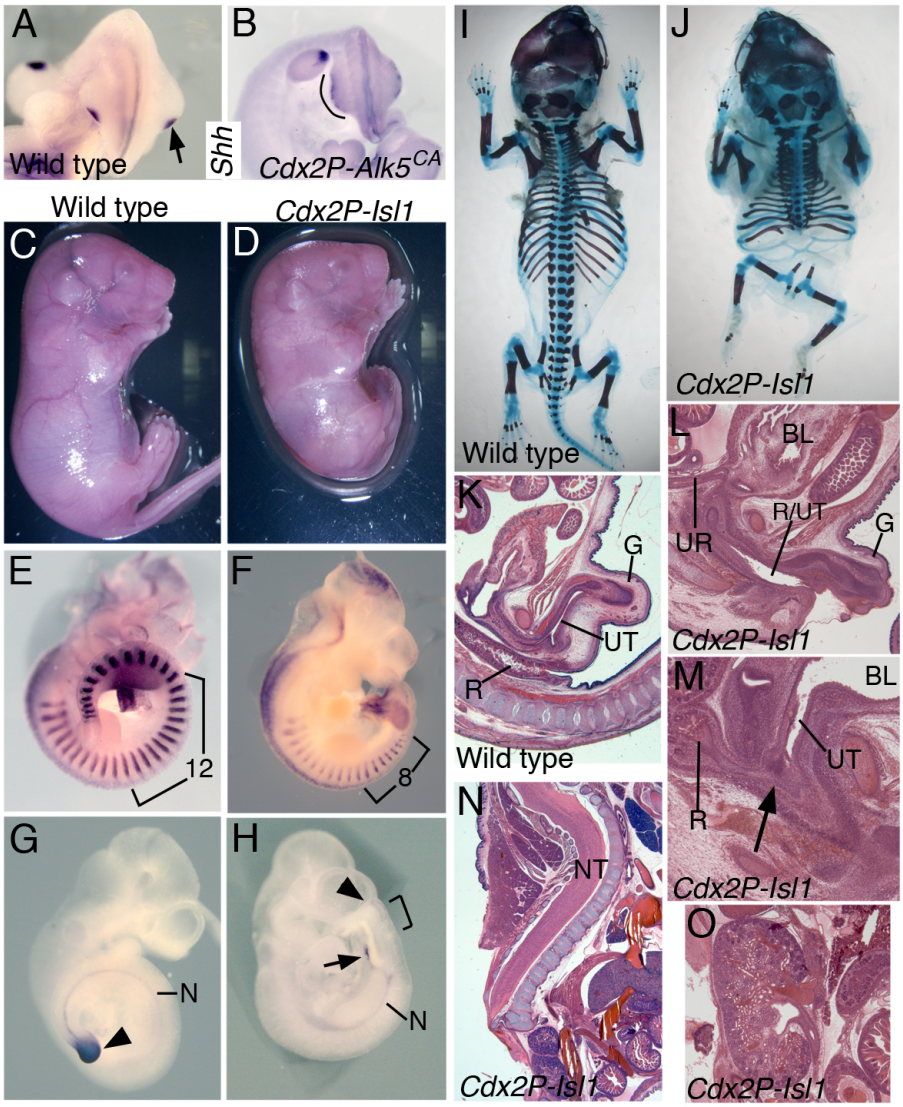
A
Wild type
Shh
B
Cdx2P-Alk5CA
Wild type
Cdx2P-Isl1
C
D
E
12
F
8
G
N
H
N
I
Wild type
J
Cdx2P-Isl1
K
G
UT
R
Wild type
L
BL
UR
R/UT
G
Cdx2P-Isl1
M
BL
UT
R
Cdx2P-Isl1
N
NT
Cdx2P-Isl1
O
Cdx2P-Isl1

Figure 5

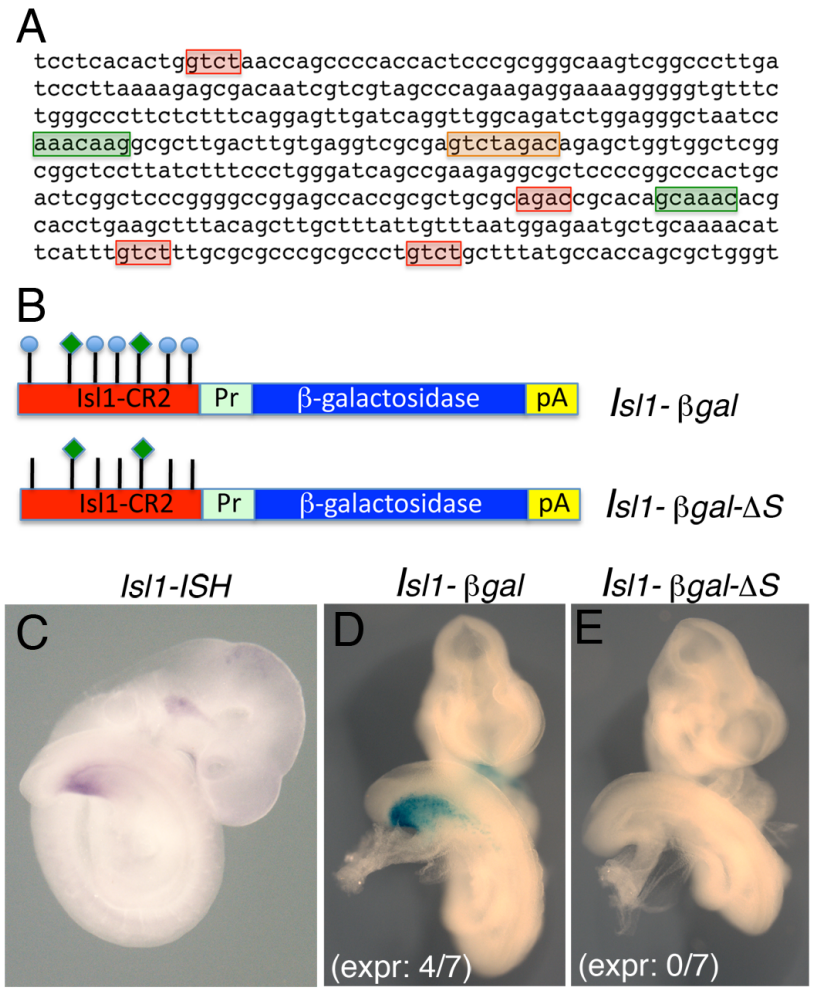
A
tcctcacactggtctaaccagccccaccactcccgcgggcaagtcggcccttga
tcccttaaaagagcgacaatcgtcgtagcccagaagaggaaaaggggtgtttc
tgggcccttctctttcaggagttgatcaggttggcagatctggagggctaatcc
aaacaaggcgcttgacttgtgaggtcgcgagtctagacagagctggtggctcgg
cggctccttatctttccctgggatcagccgaagaggcgctccccggcccactgc
actcggctcccggggccggagccaccgcgctgcgcagaccgcacagcaaaacacg
cacctgaagctttacagcttgctttattgtttaatggagaatgctgcaaaacat
tcatttgtcttgcgcgcccgcgccctgtctgctttatgccaccagcgctgggt
B
Isl1-CR2
Pr
β-galactosidase
pA
Isl1- βgal
Isl1-CR2
Pr
β-galactosidase
pA
Isl1- βgal-ΔS
Isl1-ISH
Isl1- βgal
Isl1- βgal-ΔS
C
D
(expr: 4/7)
E
(expr: 0/7)

Figure 6

SUPPLEMENTARY FIGURES

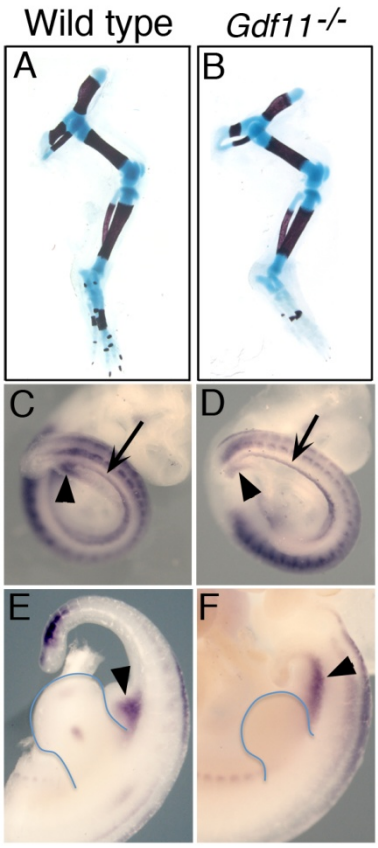

Figure S1 (related to Fig.1). Phenotypes of *Gdf11* mutant embryos. A, B. Hindlimb skeletons of E18.5 wild-type (A) and *Gdf11* mutant (B) fetuses. C-F. *Raldh2* expression in wild-type (C, E) and *Gdf11* mutant (D, F) embryos at E9.5 (C, D) or E11.5 (E, F). The arrows indicate expression in the intermediate mesoderm and the arrowheads indicate the mesodermal component of the developing cloaca.

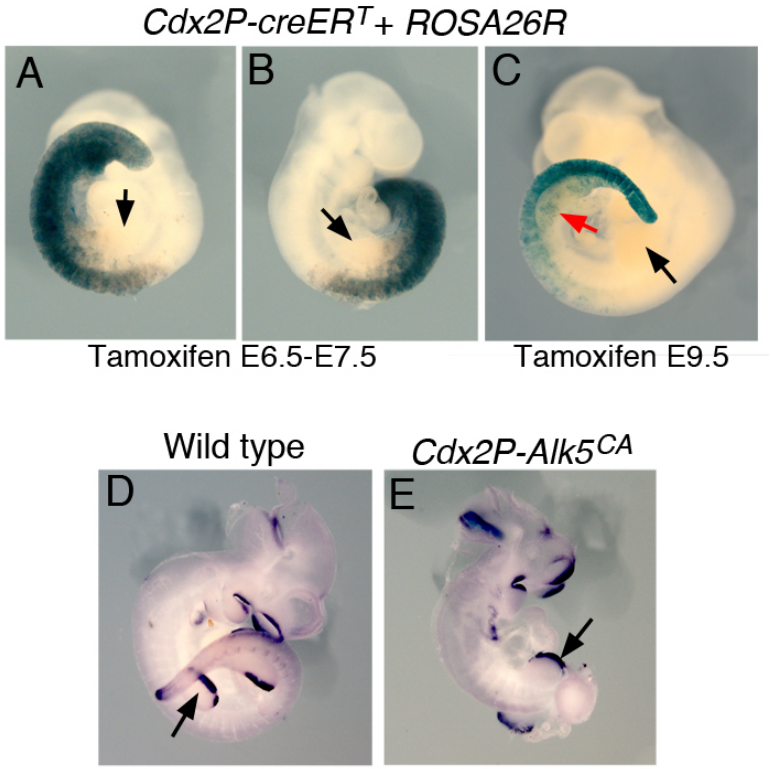

Figure S2 (related to Fig. 2). A-C. Activity of the *Cdx2P* enhancer. The activity of the enhancer was estimated by crossing a *Cdx2P-creER^T* transgenic line with the reporter *ROSA26R*. Cre activity was induced by tamoxifen administration at E6.5 and E7.5 (A,B) or at E9.5 (C). The embryos were recovered and stained for β-galactosidase at E9.5 (A, B) or E10.5 (C). Recombination was first detected only at the level of the forelimb despite tamoxifen having been administered during formation of more anterior embryonic areas, suggesting lack of *Cdx2P* activity anterior to the forelimbs. Caudal to this region, all neural and mesodermal tissues were labeled. A and B show two different views of the same embryo to facilitate observation of both expression in the caudal embryo and the position of the forelimb bud (black arrow), which is mostly negative for β-galactosidase. Tamoxifen injection at E9.5 was used to discern to which extent the wide staining observed in A and B resulted from *Cdx2P*-driven activity in neural and mesodermal derivatives or from recombination in the progenitors of the epiblast that was then stably transmitted to their derived tissues. The observation that under this induction condition activation was achieved only in more caudal embryonic areas, which coincided with the area of axial extension after tamoxifen injection, supports the conclusion of activity being mainly in the progenitors. The red arrow indicates the position of the hindlimb, which contains just a few labeled cells. **D,E. Axial truncation in *Cdx2P-Alk5^{CA}* embryos.** Wild type (D) and *Cdx2P-Alk5^{CA}* transgenic (E) embryos stained for *Fgf8* expression. The transgenic embryo was fairly normal up to the forelimb bud (arrow), but failed to extend further than this axial level.

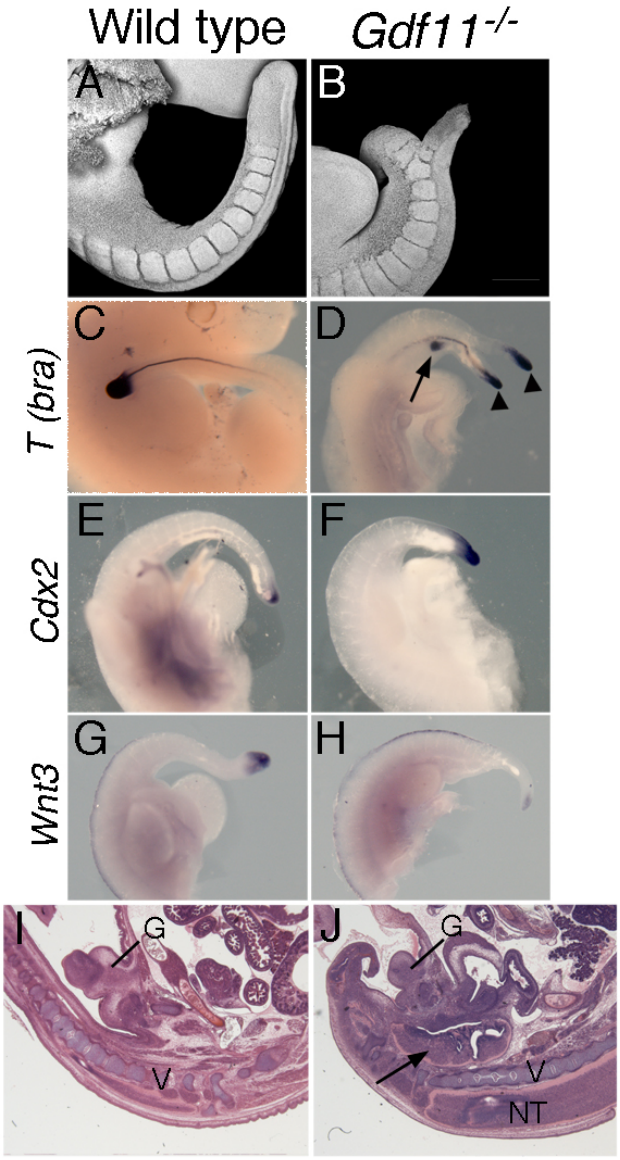

Figure S3 (related to Fig. 3). Tail phenotypes of *Gdf11* mutant embryos. A, B. Gross morphology of the tail of a wild type (A) and a Gdf11 mutant (B) embryo at E11.5. The mutant embryo has a split tail. C, D. *T* expression in E11.5 wild type (C) and *Gdf11* mutant (D) embryo with a split tail. The arrowheads indicate the tips of the split tails and the arrow an ectopic ventral expression domain next to the hindlimbs. E, F. *Cdx2* expression in E11.5 wild-type (E) and *Gdf11* mutant (F) embryos. G, H. *Wnt3a* expression in E11.5 wild-type (G) and *Gdf11* mutant (H) embryos. I, J. Sagittal sections showing the posterior region of a wild type (I) and a *Gdf11* mutant (J) embryo. The arrow indicates the ectopic neural tissue ventral to the vertebral column. V: vertebral column; NT: neural tube; G: genital tuberculum.

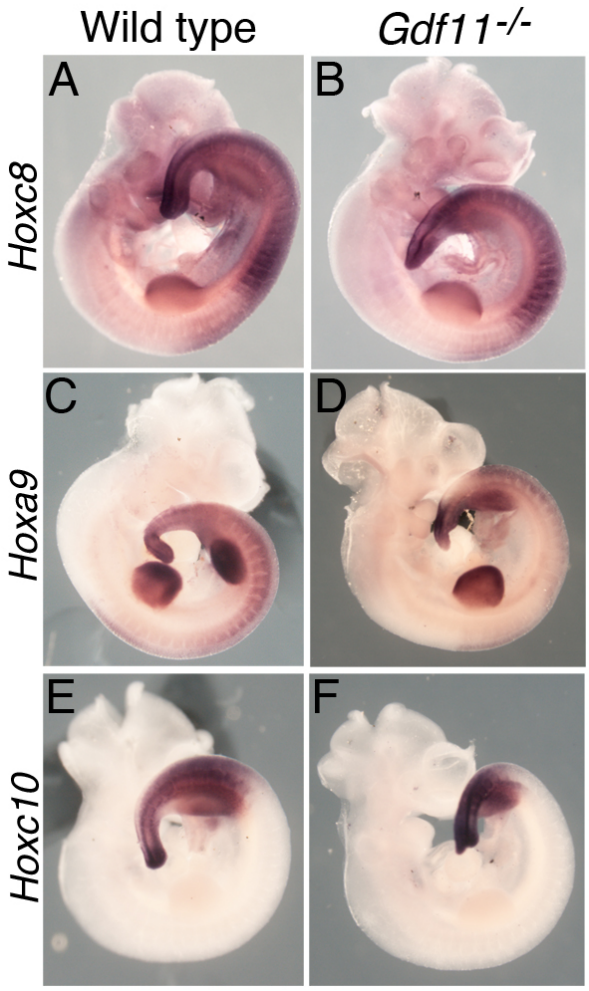

Figure S4 (related to Fig. 4). Analysis of Hox gene expression in *Gdf11* mutant embryos. Wild-type (A, C, E) and *Gdf11* mutant (B, D, F) embryos were analyzed with *Hoxc8* (A, B), *Hoxa9* (C, D), and *Hoxc10* (E, F) at E10.5. The anterior expression border of *Hoxc8* in *Gdf11* mutants is similar to that in wild type embryos. The anterior expression borders for *Hoxa9* and *Hoxc10* are posteriorly displaced in *Gdf11* mutant embryos following the relocation of the hindlimb.

Table S1 (related to Fig. 4). Summary of transgenics obtained over-expressing Hox genes in the axial progenitors.

Construct	Number of transgenics[&]		
	E10.5	E18.5	total
Cdx2P-Hoxb9	10 (2)*	7 (3)*	17 (5)*
Cdx2P-Hoxa10	10 (0)	6 (0)	16 (0)
Cdx2P-Hoxc10	6 (0)	-	6 (0)
Cdx2P-Hoxa11	8 (0)	7 (0)	15 (0)
Cdx2P-Hoxb9 + Cdx2P-Hoxa10	9 (0)	-	9 (0)
Cdx2P-Hoxb9 + Cdx2P-Hoxa11	6 (0)	-	6 (0)

[&] Indicated in parenthesis is the number of transgenics in which we observed alteration in the hindlimb position.

* Anteriorization of the hindlimb position by one segment.

SUPPLEMENTARY METHOD

Analysis of external morphology using hydrochloric carmine staining (based on Machado-Silva et al., 1998)

Embryos were dissected out and fixed overnight in 4% paraformaldehyde (made in PBS) at 4ºC. Fixed embryos were then washed twice in PBS containing 0.1% Tween 20 (PBT) at room temperature and then brought to 100% methanol through a methanol/PBT series. Dehydrated embryos were then incubated in 75% methanol (made in PBT) at room temperature before staining overnight with a 2% solution of carmine powder in 70% ethanol/2% chlorine acid in the dark at room temperature with constant shaking. Embryos were then washed quickly in 5% acid ethanol and dehydrated again in 100% methanol. Images were taken at this stage with a Zeiss StereroLumar scope. In addition, embryos were subsequently transferred to methyl salicylate through a graded series of methyl salicylate in methanol and imaged by laser scanning confocal microscopy (Zeiss LSM-510 Meta).